

## Chapter-3

# A PERTURBATIVE CORRECTION ON ELECTRON-INERTIA IN MAGNETIZED PLASMA SHEATHS

***Abstract:** An analytic hydrodynamic model<sup>†</sup> to study the equilibrium properties of planar plasma sheaths (spatially-flat geometry) in two-component quasi-neutral magnetized plasmas is proposed. It includes weak but finite electron-inertia incorporated via a regular perturbation on electronic fluid dynamics only relative to a new smallness parameter,  $\delta$ , assessing the weak inertial-to-electromagnetic coupling strength. The zeroth-order perturbation around  $\delta$  leads to the usual Boltzmann distribution law (inertialess electrons); whereas, the next higher-order correction yields the modified Boltzmann law (inertial electrons). It is seen that the mutualistic action of electron-inertia amid gyro-kinetic effects slightly modifies the local Bohm criterion with an enhancement in the ion-flow Mach threshold value (typically,  $M_{i0} \geq 1.140$ , against the traditional ‘unity’). The various electro-dynamical sheath-response features are numerically illustrated alongside future scope.*

### 3.1 INTRODUCTION

The effect of electron-inertia is normally neglected in the traditional study of plasma sheath structure and its evolutionary dynamics. In a panoptic sense, the existing theory of plasma sheaths is based on the assumption that electron-to-ion mass ratio asymptotically goes to zero [1-3]. However, although very small relative to ionic inertia, electron-inertia has been reported to have interesting influences in rendering the transonic plasma zone resonantly destabilized amid acoustic wave fluctuations [4-8]. It has, in other words, been found both theoretically and experimentally that, electron-inertia plays as a source of acoustic wave instability in the transonic plasma equilibrium conditions because of an incomplete Debye screening (due to electron-inertia) in normal plasma configurations [4-7].

<sup>†</sup>Gohain, M. and Karmakar, P. K. A perturbative correction for electron-inertia in magnetized sheath structures. *European Physical Journal D*, 70:222(1-6), 2016.

In addition to above, it has later been revealed in magnetized plasma systems that magnetic field plays an important role in controlling the kinetic energy of ions reaching the wall. As a result, the role of the field in modifying the sheath width and other characteristics needs to be well investigated [9]. The importance of such sheaths is essentially realizable for many technological applications as well [2, 9-11]. To name a few on the laboratory scales, it includes plasma processing of materials, mass-spectrometry, plasma sputtering, plasma etching, plasma-wall interactions in many fusion confinement devices, etc.

The present chapter compiles a theoretical hydrodynamic model to see the sheath structural characteristics in two-component quasi-neutral magnetized plasmas in the presence of weak but finite electron-inertia in the framework of a regular perturbative analysis in a modified form. The electronic dynamics is accordingly shown to follow different inertia-governed distribution laws with respect to the perturbation parameter derived self-consistently on the basis of small inertia-electromagnetic coupling strength. It is demonstrated, alongside diverse parametric dependences of the sheath, that putative electron-inertia amid gyro-kinetic effects slightly enhances the ion-flow threshold value (Bohm condition,  $M_{i0} \geq 1.140$ ) against the conventional *threshold unity* towards the sheath entrance.

### **3.2 PLASMA MODEL AND FORMALISM**

A hydrodynamic model configuration of magnetized collisionless plasma with presumed global quasi-neutrality is considered. The model is configured on one-dimensional (1-D) coordinate space and three-dimensional (3-D) phase space. It consists of isothermal electrons (lighter, Boltzmann distribution) and isothermal ions (heavier, fluid). Active inertial dynamics of electrons through the consideration of weak but finite electron-inertia, incorporated via a regular reductive perturbation technique [4], is incorporated to fulfil the transonic plasma behavior [5-7]. The external magnetic field is embedded in the  $(x-z)$  plane and makes an angle  $\theta$  with respect to the  $x$ -direction (bulk flow). We consider both magnetized electrons and magnetized ions rather than the conventional viewpoint of treating electrons as unmagnetized species in similar plasma environments [12-14]. A schematic diagram of our considered magnetized plasma sheath configuration together with various directed parametric fields is displayed in figure 3.1.

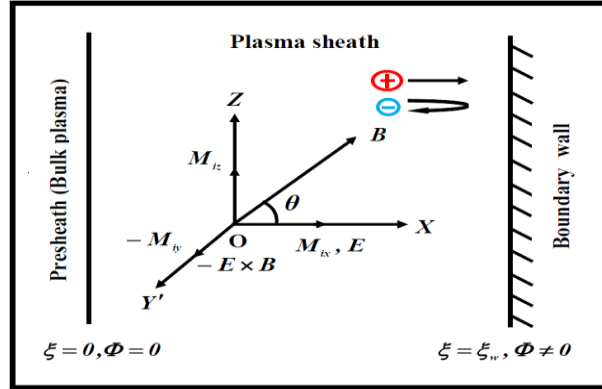


Figure 3.1: Schematic of the considered plasma sheath configuration, same as figure 2.1.

The different relevant physical parameters here are normalized by adopting a standard normalization scheme [8] which is shown in Table 3.1.

Table 3.1: Standard normalization scheme

S No.	Physical parameters	Normalizing parameters
1	Position ( $\xi$ )	Plasma Debye length ( $\lambda_{De}$ )
2	Population density ( $N_e, N_i$ )	Equilibrium density ( $n_{e0}, n_{i0}$ )
3	Mach number ( $M_e, M_i$ )	Sound phase speed ( $c_s$ )
4	Electric potential ( $\Phi$ )	Plasma thermal potential ( $T_e/e$ )

The basic set of the normalized equations [15] governing equilibrium magnetized plasma (time-stationary) is developed as follows. According to the Boltzmann distribution, electron number density in the thermalized state in the asymptotically zero-limit of electron-to-ion mass ratio ( $m_e/m_i \rightarrow 0$ ) with all usual notations (discussed later) is set out as

$$N_{e0} = \exp(-\Phi_0). \quad (3.1)$$

The electron continuity and momentum equations in the steady-state form ( $\partial/\partial t \sim 0$ ) in the same customary system of notations are respectively given as

$$\frac{\partial}{\partial \xi}(N_e M_e) = 0, \quad (3.2)$$

$$\left(\frac{m_e}{m_i}\right) M_e \left(\frac{\partial M_e}{\partial \xi}\right) = -\frac{\partial \Phi}{\partial \xi} - \frac{1}{N_e} \frac{\partial N_e}{\partial \xi} - \frac{1}{N_e} \left(\frac{1}{n_0} M_{ey} \alpha \sin \theta\right). \quad (3.3)$$

The physical parameters are assumed to vary only in the  $x$ -direction, for which  $\vec{\nabla} \rightarrow \hat{x} \partial / \partial x$ , and so the other remaining components are justifiably omitted. The direction of the magnetic field is taken as  $\hat{B} = \vec{B} / |\vec{B}| = (\hat{x} \cos \theta + \hat{z} \sin \theta)$ , where  $\theta$  is the angle of  $\vec{B}$  relative to the bulk flow. Obviously, the small terms in equation (3) are the electronic inertial force term,  $T_e = (m_e / m_i) M_e (\partial M_e / \partial \xi)$ , and the Lorentz force term  $T_L = [1 / N_e ((1 / n_0) M_{ey} \alpha \sin \theta)]$ . We now estimate their relative strengths in the parametric space of laboratory plasmas [8, 15] as:  $M_{ey} = 10^{-1}$ ,  $\partial M_e / \partial \xi = 10^{-15}$ ,  $B = 0.1$  T,  $m_e = 9.1 \times 10^{-31}$  kg,  $m_i = 1.67 \times 10^{-27}$  kg,  $e = 1.6 \times 10^{-19}$  C,  $n_0 = 10^{19} \text{ m}^{-3}$ ,  $\varepsilon = 8.854 \times 10^{-12} \text{ F m}^{-1}$  and  $\theta = 30^\circ$ . In such conditions,  $T_e \sim 10^{-19} (M_e)$  and  $T_L \sim 10^{-23} (1 / N_e)$ , too meager to affect electron dynamics. A smallness parameter,  $\delta$ , is therefore introduced for a perturbative expansion of electron inertial dynamics as

$$\left(\frac{m_e}{m_i}\right) M_e \left(\frac{\partial M_e}{\partial \xi}\right) \approx \delta, \quad (3.4)$$

$$\frac{1}{N_e} \left(\frac{1}{n_0} M_{ey} \alpha \sin \theta\right) \approx \delta. \quad (3.5)$$

The relevant parameters,  $N_e$  and  $\Phi$ , are expanded perturbatically around  $\delta$  as follows

$$\left. \begin{aligned} N_e &= N_{e0} + \delta N_{e1} + \delta^2 N_{e2} + \dots, \\ \Phi &= \Phi_0 + \delta \Phi_1 + \delta^2 \Phi_2 + \dots. \end{aligned} \right\} \quad (3.6)$$

Substituting equations (3.4), (3.5) and (3.6) in equation (3.3) simultaneously and retaining the terms up to the first order, we have

$$\delta = -\frac{\partial \Phi_0}{\partial \xi} - \delta \frac{\partial \Phi_1}{\partial \xi} - \frac{1}{N_{e0}} \frac{\partial N_{e0}}{\partial \xi} - \delta \frac{1}{N_{e0}} \frac{\partial N_{e1}}{\partial \xi} + \delta N_{e1} \frac{1}{N_{e0}^2} \frac{\partial N_{e0}}{\partial \xi} + \delta^2 N_{e1} \frac{1}{N_{e0}^2} \frac{\partial N_{e1}}{\partial \xi} - \delta. \quad (3.7)$$

Equating the like terms in various powers of  $\delta$  from both sides of equation (3.7), one obtains

$$O(\delta^0): -\frac{\partial \Phi_0}{\partial \xi} - \frac{1}{N_{e0}} \frac{\partial N_{e0}}{\partial \xi} = 0, \quad (3.8)$$

$$O(\delta^1): 1 = -\frac{\partial\Phi_1}{\partial\xi} - \frac{1}{N_{e0}} \frac{\partial N_{e1}}{\partial\xi} + N_{e1} \frac{1}{N_{e0}^2} \frac{\partial N_{e0}}{\partial\xi} - 1, \text{ and so forth.} \quad (3.9)$$

Now, equations (3.8) and (3.9), on further integration and simplification, yield

$$N_{e0} = \exp(-\Phi_0). \quad (3.10)$$

It is seen from equation (3.10) that the zeroth-order perturbation reproduces the Boltzmann distribution law for electrons. We now apply a current specially imposed condition for simplification as  $\partial N_{e0}/\partial\xi \rightarrow 0$  (small equilibrium-gradient approximation) so that the term

$(N_{e1}/N_{e0}^2)(\partial N_{e0}/\partial\xi) \rightarrow 0$  in equation (3.9). As a result, integration of equation (3.9) yields

$$N_{e1}(\xi) = -(\Phi_1 + 2\xi)\exp(-\Phi_0). \quad (3.11)$$

Equation (3.11) represents the inertia-corrected electron population distribution law (inertia-modified Boltzmannian) of our current investigative interest. In order for further simplification of our problem, we choose  $\Phi_0 \approx \Phi_1 \sim \Phi$ . On potential differentiation, equation (3.11) gives

$$\frac{\partial N_{e1}}{\partial\Phi} = -\exp(-\Phi) \left[ 1 - \Phi - 2\xi + 2 \frac{\partial\xi}{\partial\Phi} \right]. \quad (3.12)$$

The ion continuity and momentum equations under the isothermal pressure law,  $p_i = \gamma T_i n_i$ , are respectively presented as

$$N_i M_{ix} = M_{i0}, \quad (3.13)$$

$$M_{ix} \frac{\partial M_{ix}}{\partial\xi} = \frac{\partial\Phi}{\partial\xi} + M_{iy} \alpha \sin\theta - \frac{\gamma}{\sigma} \frac{1}{N_i} \frac{\partial N_i}{\partial\xi}. \quad (3.14)$$

Here,  $\sigma = T_e/T_i$  is the electron-to-ion temperature ratio (both in eV), with  $\alpha = \omega_{ci}/\omega_{pi}$  as the ratio of the ion cyclotron frequency  $\omega_{ci} = eB/m_i$  and plasma frequency  $\omega_{pi} = \sqrt{n_0 e^2 / \epsilon m_i}$ .

Lastly, the electrostatic Poisson equation, coupling electron-ion dynamics in a closure, is given as

$$\frac{\partial^2\Phi}{\partial\xi^2} = N_i - N_{e1}. \quad (3.15)$$

Now, substituting  $M_{ix} = M_{i0}/N_i$  from equation (3.13) in equation (3.14), we have

$$M_{iy} \alpha \sin \theta = -\frac{M_{i0}^2}{N_i^3} \frac{\partial N_i}{\partial \xi} + \frac{M_{i0}}{N_i^2} \frac{\partial M_{i0}}{\partial \xi} - \frac{\partial \Phi}{\partial \xi} + \frac{\gamma}{\sigma} \frac{1}{N_i} \frac{\partial N_i}{\partial \xi}. \quad (3.16)$$

Multiplying both sides with  $(\partial \Phi / \partial \xi)^{-1}$  and simplifying, equation (3.16) yields

$$\frac{\partial N_i}{\partial \Phi} = -\left[1 + M_{iy} \alpha \sin \theta \left\{ \frac{\partial \Phi}{\partial \xi} \right\}^{-1} \right] \left\{ \left( \frac{M_{i0}^2}{N_i^3} - \frac{\gamma}{\sigma} \frac{1}{N_i} \right)^{-1} \right\}. \quad (3.17)$$

Differentiating equation (3.15) with respect to  $\Phi$ , and substituting  $\partial N_{e1} / \partial \Phi$  from equation (3.12) and  $\partial N_i / \partial \Phi$  from equation (3.17), one finds

$$\frac{\partial}{\partial \Phi} \left( \frac{\partial^2 \Phi}{\partial \xi^2} \right) = -\left[1 + M_{iy} \alpha \sin \theta \left\{ \frac{\partial \Phi}{\partial \xi} \right\}^{-1} \right] \left\{ \left( \frac{M_{i0}^2}{N_i^3} - \frac{\gamma}{\sigma} \frac{1}{N_i} \right)^{-1} \right\} - \exp(-\Phi) \left[1 - \Phi - 2\xi + 2 \frac{\partial \xi}{\partial \Phi} \right]. \quad (3.18)$$

After integrating, equation (3.18) can be expressed as

$$\left( \frac{\partial^2 \Phi}{\partial \xi^2} \right) = -\int \left[1 + M_{iy} \alpha \sin \theta \left\{ \frac{\partial \Phi}{\partial \xi} \right\}^{-1} \right] \left\{ \left( \frac{M_{i0}^2}{N_i^3} - \frac{\gamma}{\sigma} \frac{1}{N_i} \right)^{-1} \right\} - \exp(-\Phi) \left[1 - \Phi - 2\xi + 2 \frac{\partial \xi}{\partial \Phi} \right] \partial \Phi. \quad (3.19)$$

At the sheath edge,  $\Phi = (-e\phi/T_e)$  should be minimum so that a smooth, non-oscillatory and monotonic transition of the plasma from presheath to sheath region takes place [3]. Thus, the condition for minimizing the potential at the sheath edge,  $\Phi = \Phi_{\min}$ , for the monotonous variation, requires the following derived condition on the potential curvature [15] as

$$\left( \frac{\partial^2 \Phi}{\partial \xi^2} \right) \geq 0. \quad (3.20)$$

Therefore, from equation (3.19), one gets

$$-\int \left[1 + M_{iy} \alpha \sin \theta \left\{ \frac{\partial \Phi}{\partial \xi} \right\}^{-1} \right] \left\{ \left( \frac{M_{i0}^2}{N_i^3} - \frac{\gamma}{\sigma} \frac{1}{N_i} \right)^{-1} \right\} - \exp(-\Phi) \left[1 - \Phi - 2\xi + 2 \frac{\partial \xi}{\partial \Phi} \right] \partial \Phi \geq 0, \quad (3.21)$$

which, on the  $\Phi$ -differentiation on both sides, yields

$$-\frac{\partial}{\partial \Phi} \int \left[1 + M_{iy} \alpha \sin \theta \left\{ \frac{\partial \Phi}{\partial \xi} \right\}^{-1} \right] \left\{ \left( \frac{M_{i0}^2}{N_i^3} - \frac{\gamma}{\sigma} \frac{1}{N_i} \right)^{-1} \right\} - \exp(-\Phi) \left[1 - \Phi - 2\xi + 2 \frac{\partial \xi}{\partial \Phi} \right] \partial \Phi \geq 0. \quad (3.22)$$

Thus, according to standard rule of basic integration [16], equation (3.22) gives

$$-\left[1 + M_{iy} \alpha \sin \theta \left\{ \frac{\partial \Phi}{\partial \xi} \right\}^{-1} \right] \left\{ \left( \frac{M_{i0}^2}{N_i^3} - \frac{\gamma}{\sigma} \frac{1}{N_i} \right)^{-1} \right\} + \exp(-\Phi) \left[ 1 - \Phi - 2\xi + 2 \frac{\partial \xi}{\partial \Phi} \right] \geq 0. \quad (3.23)$$

The boundary conditions,  $\Phi \rightarrow 0$ ,  $N_i \rightarrow 1$  and  $\partial \Phi / \partial \xi \neq 0$ , hold good at the sheath edge. Thus, applying the condition for monotonic potential transition in equation (3.23), the local *Bohm criterion* needed for *sheath formation* in a bounded plasma system comes out as

$$M_{i0} \geq \left[ \frac{1}{\left\{ 1 - 2\xi + 2 \left( \frac{\partial \xi}{\partial \Phi} \right)_{\Phi=0} \right\}} \left\{ 1 + M_{iy} \alpha \sin \theta \left( \frac{\partial \Phi}{\partial \xi} \right)_{\Phi=0}^{-1} \right\} + \left( \frac{\gamma}{\sigma} \right) \right]^{1/2}. \quad (3.24)$$

It is clearly seen that the new Bohm condition, which usually states that the threshold value of the ion Mach number near the sheath entrance should be at least equal to unity, gets drastically modified due to the joint role of weak but finite electron-inertial perturbation via  $\left\{ 1 - 2\xi + 2 \left( \frac{\partial \xi}{\partial \Phi} \right)_{\Phi=0} \right\}^{-1/2}$ , magnetic field via  $\alpha$ , and the thermal motion of ions via  $\sigma = T_e / T_i$ . It is interesting to note that, once the new factors considered here are switched off, equation (24) reduces to the well-established Bohm criterion,  $M_{i0} \geq 1$  [2, 3].

### 3.3 RESULTS

An analytical model to study the time-stationary behavior of plasma sheath formation in a collisionless quasi-neutral warm plasma configuration in the presence of the lowest-order electron-inertial perturbative correction and oblique magnetic field is investigated. The local Bohm criterion is systematically derived and special corollaries are discussed. It is seen that the lowest-order electron-inertial correction, in the presence of the Lorentz gyro-kinetic effects, plays a crucial role in the sheath evolution. The ion threshold Mach number near the sheath edge is slightly enhanced with respect to the normal Bohm value of unity. We now consider laboratory plasma parameter values [15, 17] like  $M_{iy} = 10^{-2}$ ,  $B = 0.1$  T,  $n_0 = 10^{19} \text{ m}^{-3}$ ,  $\varepsilon = 8.854 \times 10^{-12} \text{ F m}^{-1}$ ,  $\theta = 30^\circ$ ,  $M_{e0} = 1$ ,  $\gamma = 1$ ,  $\sigma = T_e / T_i = 3.33$  and  $(\partial \Phi / \partial \xi)_{\Phi=0} = 0.42 \times 10^6$ . In such situations, the new Bohm condition gives the threshold Mach value as  $M_{i0} \geq 1.140$ .

A numerical analysis is carried out by applying the fourth-order Runge-Kutta method [18] to see the exact evolutionary patterns of the sheath structure. The numerical profiles,

thus obtained, are displayed graphically in figures 3.2-3.3. Figure 3.2 illustrates the spatial profiles of the normalized (a) electrostatic potential ( $\Phi$ ), and (b) electrostatic potential curvature ( $\partial^2\Phi/\partial\xi^2$ ) under different strengths of the applied magnetic field ( $B=0.10, 0.20$  and  $0.30$  T). The different input initial values [8, 15] used are  $\xi_i = 0.01$  with  $\Delta\xi = 0.01$ ,  $N_{e0} = 1$ ,  $N_{i0} = 1$ ,  $M_{ix0} = 10^{-1}$ ,  $(\Phi)_i = -1 \times 10^{-2}$  and  $(\Phi_{\xi\xi})_i = -1 \times 10^{-3}$ . The other fixed inputs [8, 15] are  $M_{e0} = 1$ ,  $M_{i0} = 1$ ,  $M_{iy0} = 10^{-2}$ ,  $n_0 = 1 \times 10^{19} \text{ m}^{-3}$ ,  $\alpha = 2.30 \times 10^{-3}$ ,  $\gamma = 1$ ,  $\sigma = 1 \text{ eV}$  and  $\theta = 30^\circ$ . It is seen that  $\Phi$  and  $\partial^2\Phi/\partial\xi^2$  go on increasing with increase in the magnetic field. This is because of enhanced ion gyro-kinetic effects producing a new equilibrium. The gyro-kinetic influence is more for larger  $B$ ; and vice-versa. It is realized that  $B$  plays an important role in holding up ions gyro-kinetically moving towards the sheath region. The electron-ion density separation is evident from figure 3.2(b). It is seen that, with increasing  $B$ , the deviation from quasi-neutrality increases depicting non-neutral sheath.

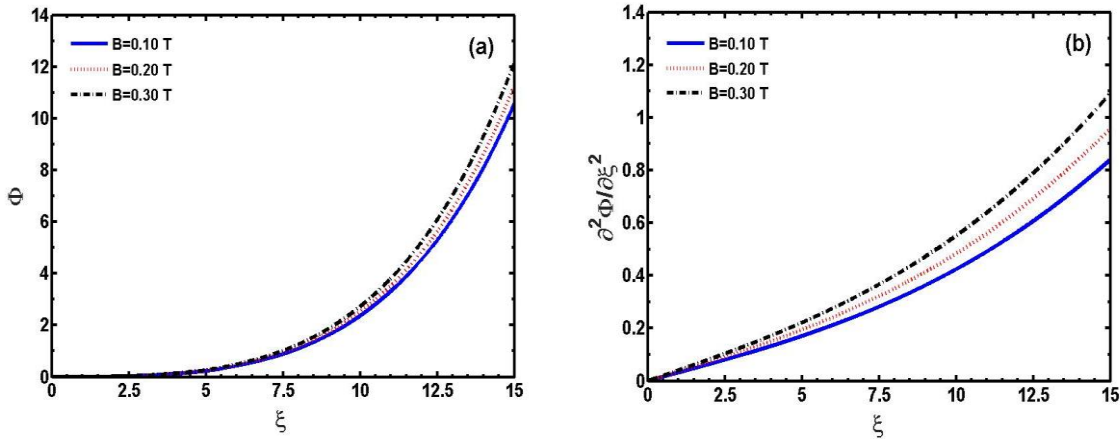


**Figure 3.2:** The spatial profiles of the normalized (a) electrostatic potential ( $\Phi$ ), and (b) electrostatic potential curvature ( $\partial^2\Phi/\partial\xi^2$ ) as a measure of deviation from quasi-neutrality under the different  $B$ -values. Different lines link to  $B = 0.10$  T (blue),  $0.20$  T (red), and  $0.30$  T (black); respectively. The related fine details are presented in the text.

Figure 3.3 depicts the same as figure 3.2, but with  $B = 0.30$  T (fixed). Different lines now correspond to  $\theta = 10^\circ, 30^\circ$ , and  $50^\circ$ ; respectively. The evolutionary sheath patterns in this case are found to be consistent with those as in figure 3.2.



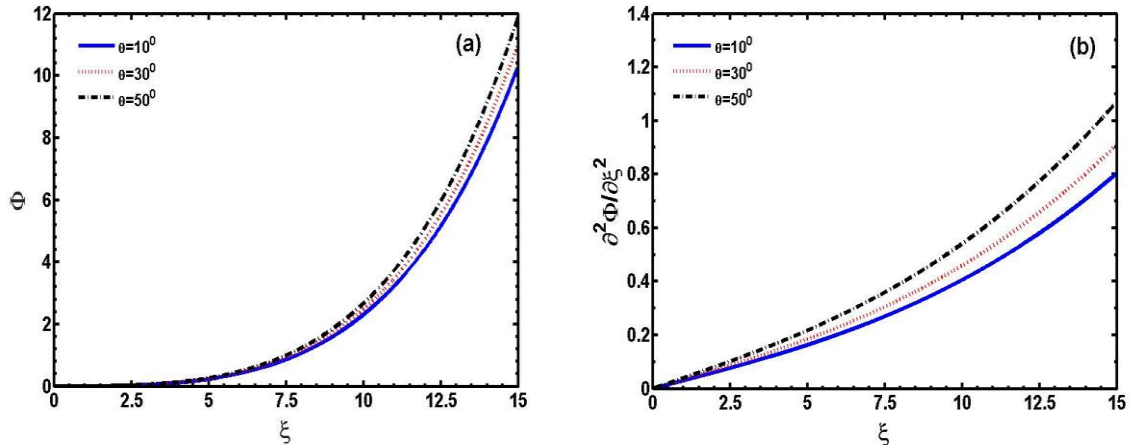


**Figure 3.3:** Same as figure 3.2, but with  $B = 0.20$  T (fixed). Different lines correspond to  $\theta = 10^\circ$ ,  $30^\circ$ , and  $50^\circ$ ; respectively.

### 3.4 CONCLUSIONS

A hydrodynamic model is theoretically formulated to study the equilibrium structural properties of steady-state plasma sheaths in a magnetized plasma configuration. It accounts for the lowest-order perturbative electron-inertial correction. The effects of electron-inertia, applied magnetic field and its orientation are found to play an important role in influencing the sheath dynamics parametrically. To sum up, the main concluding remarks are given as

1. The local Bohm criterion is revisited in quasi-neutral magnetized collisionless plasmas in the presence of electron-inertial perturbative dynamics.
2. The ion flow threshold value entering the sheath edge is found to be enhanced due to the considered paramount factors (via modified Bohm criterion).
3. We see that the potential and its curvature increase with increase in the applied magnetic field and the field orientation.
4. It is found that, at the sheath edge, the deviation from quasi-neutrality is more pronounced for higher magnetic field and for greater field-flow angle.
5. The sheath structure investigated here can be intimately related with ion-acoustic shock development, because a travelling sheath would pertain to shock wave propagation, despite dissimilar boundary conditions. It may, thus, provide an alternative modified sheath-based viewpoint of hydrodynamic shocks and their evolutionary dynamics.
6. The theoretical analysis is based on two distinct isothermal electron-ion fluids, against a recent hydro-kinetic study showing that at the vicinity of the sheath edge, the ion temperature

may change appreciably [19]. We admit that the inclusion of non-isothermal constituent fluids with proper equations of state is more suitable to understand real sheath structure.

It is, lastly, recognized that a collisionless plasma configuration is realistically improper and inadequate as well. This is because the collisions between ions and neutrals could play a decisive role in influencing the effects of magnetic field on the upper and lower limits of the Bohm sheath criterion [20]. Thus, a more in-depth study of the plasma sheath in the presence of all the possible collisional transport effects needs to be formulated.

## REFERENCES

- [1] Bohm, D. *The Characteristics of Electrical Discharges in Magnetic Fields*. edited by Guthrie, A. and Wakerling, R. McGraw-Hill, New York, 1949.
- [2] Stangeby, P. C. *The Plasma Boundary of Magnetic Fusion Devices*, IOP Publishing Ltd., Bristol and Philadelphia, 2000.
- [3] Riemann, K. U. The Bohm criterion and sheath formation. *Journal of Physics D: Applied Physics*, 24:493-518, 1991.
- [4] Karmakar, P. K., Deka, U., and Dwivedi, C. B. Graphical analysis of electron inertia induced acoustic instability. *Physics of Plasmas*, 12:032105(1-9), 2005.
- [5] Karmakar, P. K. and Dwivedi, C. B. Analytical integrability and physical solutions of d-KdV equation. *Journal of Mathematical Physics*, 47:032901(1-17), 2006.
- [6] Karmakar, P. K., Deka, U., and Dwivedi, C. B. Response to “Comment on ‘Graphical analysis of electron inertia induced acoustic instability’”. *Physics of Plasmas*, 13:104702(1-3), 2006.
- [7] Deka, U., Sarma, A., Prakash, R., Karmakar, P. K., and Dwivedi, C. B. Electron inertia delay effect on acoustic soliton behavior in transonic region. *Physica Scripta*, 69:303-312, 2004.
- [8] Deka, U. and Dwivedi, C. B. Effect of electron inertial delay on Debye sheath formation. *Brazilian Journal of Physics*, 40(3):333-339, 2010.
- [9] Chalise, R. and Khanal, R. The study of kinetic energy of ion and sheath thickness in magnetized plasma sheath. *Journal of Materials Science and Engineering A*, 5(1-2):41-46, 2015.

- [10] Zou, X., Liu, J. Y., Gong, Y., Wang, Z-X., Liu, Y., and Wang, X-G. Plasma sheath in a magnetic field. *Vacuum*, 73:681-685, 2004.
- [11] Zou, X., Qiu, M., Liu, H., Zhang, L., Liu, J., and Gong, Y. The ion density distribution in a magnetized plasma sheath. *Vacuum*, 83:205-208, 2009.
- [12] Allen, J. E. The plasma boundary in a magnetic field. *Contribution to Plasma Physics*, 48:400-405, 2008.
- [13] Hatami, M. M., Shokri, B., and Niknam, A. R. Numerical investigation of the magnetized plasma sheath characteristics in the presence of negative ions. *Physics of Plasmas*, 15:123501(1-6), 2008.
- [14] Liu, H., Zou, X., and Qiu, M. Sheath criterion for an electronegative plasma sheath in an oblique magnetic field. *Plasma Science and Technology*, 16(7):633-636, 2014.
- [15] Ou, J. and Yang, J. Properties of a warm plasma collisional sheath in an oblique magnetic field. *Physics of Plasmas*, 19:113504(1-7), 2012.
- [16] Rohde, U. L., Jain, G. C., Poddar, A. K., and Ghosh, A. K. *Introduction to Integral Calculus*. Wiley, New Jersey, 2012.
- [17] Khoramabadi, M., Ghomi, H. R., and Ghoranneviss, M. Effects of ion temperature on collisional DC sheath in plasma ion implantation. *Journal of Plasma and Fusion Research SERIES*, 8:1399-1402, 2009.
- [18] Butcher, J. C. An introduction to “Almost Runge-Kutta” methods. *Applied Numerical Mathematics*, 24:331-342, 1997.
- [19] Kuhn, S., Riemann, K. U., Jelic, N., Tskhakaya Sr., D. D., Tskhakaya Jr., D., and Stanojevic, M. Link between fluid and kinetic parameters near the plasma boundary. *Physics of Plasmas*, 13:013503(1-8), 2006.
- [20] Masoudi, S. F. and Ebrahiminejad, Zh. The sheath criterion for a collisional plasma sheath at the presence of external magnetic field. *The European Physical Journal D*, 59:421-425, 2010.